Nucleic Acids Research, 1999, Vol. 27, No. 3 **859–865**

The formation of adjacent triplex–duplex domains in DNA

Kang Hoon Nam[+], Saraswathy Abhiraman and Roger M. Wartell*

School of Biology, Georgia Institute of Technology, Atlanta, GA 30332, USA

Received August 28, 1998; Revised and Accepted December 7, 1998

ABSTRACT

The ability of single-stranded DNA oligomers to form adjacent triplex and duplex domains with two DNA structural motifs was examined. Helix–coil transition curves and a gel mobility shift assay were used to characterize the interaction of single-stranded oligomers 12–20 nt in length with a DNA hairpin and with a DNA duplex that has a dangling end. The 12 nt on the 5′-ends of the oligomers could form a triplex structure with the 12 bp stem of the hairpin or the duplex portion of the DNA with a dangling end. The 3′-ends of the 17–20 nt strands could form Watson–Crick pairs to the five base loop of the hairpin or the dangling end of the duplex. Complexes of the hairpin DNA with the single-stranded oligomers showed two step transitions consistent with unwinding of the triplex strand followed by hairpin denaturation. Melting curve and gel competition results indicated that the complex of the hairpin and the 12 nt oligomer was more stable than the complexes involving the extended single strands. In contrast, results indicated that the extended single-stranded oligomers formed Watson–Crick base pairs with the dangling end of the duplex DNA and enhanced the stability of the adjacent triplex region.

INTRODUCTION

The triple helix structure of DNA has been the focus of considerable interest for its possible biological role(s) and for its potential therapeutic applications (1,2). Intermolecular triplexes can be formed between sequence-specific oligonucleotides and their target sites on duplex DNA. An intramolecular triplex is the major structural feature of H-DNA (3–6), an unusual conformation that can occur in homopurine–homopyrimidine regions of supercoiled DNAs under physiological conditions. Triplex-based strategies for DNA recognition may have applications such as sequence-specific cleavage of chromosomal DNA (7,8) and inhibition of replication and transcription (9–16). The recognition of duplex DNA by an oligonucleotide via triplex formation shows strong dependence on environmental conditions and DNA sequence. Due to these limitations a number of approaches have been proposed to enhance triplex stability under physiological conditions. These include the use of non-natural bases or crosslinkers (17–20), change of backbone (21) and oligonucleotide intercalator conjugates (22,23).

Studies on bimolecular triplex formation have frequently employed short DNA molecules as model systems (24–30). Studies on bimolecular triplexes that model structures expected in H-DNA have employed a purine-rich oligonucleotide and a DNA molecule with two palindromic pyrimidine sequences bridged at one or both ends by a loop (27–30). In these complexes the pyrimidine strands can fold around the central purine-rich strand forming a triplex. The stability of these complexes has been shown to vary according to loop size and sequence. In the case of a pentanucleotide loop, when the purine strand did not extend across the loop, the complex was stabilized if the first and the fifth loop bases were complementary in the Watson–Crick sense (27). When the purine strand extended across the loop, stabilizing interactions occurred if either the first or fifth loop base was complementary to the first base overhang of the central strand (28). These studies indicated that adjacent triplex and duplex structures may exist without intervening sequences.

In the current work we have examined the possible formation of adjacent triplex and duplex structures between an oligonucleotide and two structural motifs, a base paired hairpin DNA molecule or a duplex DNA with a dangling single-stranded end. The former structural motif may occur in palindromic sequences of DNA, while the latter may model a region near a replicating fork. Unlike bimolecular triplexes that employ a purine strand and two pyrimidine sequences connected by a loop, the present study employs pyrimidine-rich single strands that bind to a Watson–Crick paired hairpin stem or duplex DNA with Hoogsteen base pairs. The pyrimidine strands are designed so that they have the potential to form a triplex in the duplex region of the target DNA and Watson–Crick base pairs with the loop of the hairpin DNA or the dangling end of the tailed duplex (Fig. 1a).

MATERIALS AND METHODS

Oligonucleotide synthesis

All DNA oligonucleotides were purchased from Operon Inc. and purified by HPLC with a Zorbax XDB-C8 reverse phase column (300 Å pore size) using aqueous triethylammonium acetate (100 mM, pH 7.2)/acetonitrile (7–20%) eluant and UV detection. Appropriate fractions were combined, dried *in vacuo*, dissolved in 1 ml dH_2O and desalted by passage through an NAP-10 Sephadex cartridge (Pharmacia). The oligonucleotides in the eluant samples were vacuum dried, dissolved in 0.5 ml of Tris–EDTA buffer (pH 7.0) and quantified by absorption at 260 nm. Molar extinction coefficients for the oligomers were

*To whom correspondence should be addressed. Tel: +1 404 894 3735; Fax: +1 404 894 0519; Email: roger.wartell@biology.gatech.edu

[+]Present address: Department of Biology, Yonsei University, Seoul 120-749, Korea

a

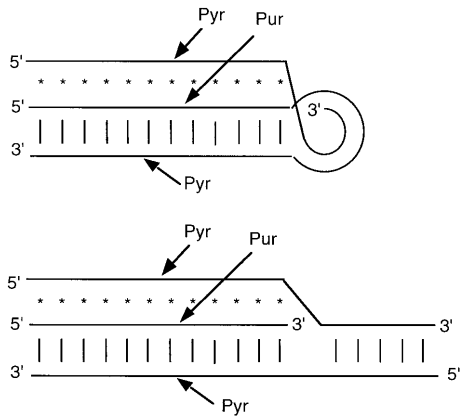

b

Pyrimidine-rich single strands

PY12	5'- CCTCTCCTCCCT- 3'
PY17	5'- CCTCTCCTCCCTAGTGA- 3'
PY18	5'- CCTCTCCTCCCTTAGTGA- 3'
PY19	5'- CCTCTCCTCCCTTTAGTGA- 3'
PY20	5'- CCTCTCCTCCCTTTAGTGAT- 3'
PY20G	5'- CCTCTCCTCCCTTTCGCGCG- 3'

Sequence of base paired structures

DX12	**R12**	5'- G G A G A G G A G G G A- 3'
	Y12	3'- C C T C T C C T C C C T- 5'
H29		5'- G G A G A G G A G G G A **T C**
		3'- C C T C T C C T C C C T **T C** **A**
DT12/6	**R12**	5'- G G A G A G G A G G G A- 3'
	Y18	3'- C C T C T C C T C C C T T C A C T A - 5'
DT12/6M	**R12**	5'- G G A G A G G A G G G A- 3'
	Y18M	3'- C C T C T C C T C C C T T T A T T A- 5'
DT12/6G	**R12**	5'- G G A G A G G A G G G A- 3'
	Y18G	3'- C C T C T C C T C C C T G C G C G C- 5'

Figure 1. (**a**) Illustration of potential DNA triplex/duplex structures investigated in this work. (**b**) Sequences of single-stranded oligonucleotides, hairpin DNA (H29) and duplex with 5′ dangling ends (DT12/6, DT12/6M and DT12/6G) used in the study. Underlined bases in the single strands indicate the regions that can form Watson–Crick base pairs with complementary bases in the H29 loop (shown in bold) or in the dangling ends of the DT12/6, DT12/6M or DT12/6G molecules.

calculated using dinucleotide absorbance data (31). All DNA oligomers utilized are shown in Figure 1b.

For gel mobility shift assays, the oligonucleotides were end-labeled with [γ-^{32}P]ATP (Amersham) using T4 polynucleotide kinase. Each oligonucleotide (10 pmol) was mixed with 5 U of T4 polynucleotide kinase in 1× T4 polynucleotide kinase buffer and each sample mixture was incubated at 37°C for at least 2 h. The unreacted [γ-^{32}P]ATP was removed by filtering the labeled sample through a QIAquick nucleotide removal column (Qiagen).

Thermal denaturation experiments

Samples characterized by thermal denaturation/renaturation curves monitored by UV absorbance contained a 1:1 molar ratio of an oligonucleotide and either the 29 nt hairpin DNA (H29) or a 12 nt:18 nt partial duplex with dangling end (e.g. DT12/6). Experiments were carried out using 1 μM each of the single strand and either the duplex or hairpin in 1× NAE (100 mM sodium acetate/acetic acid, 1 mM EDTA) at pH 5.0.

Melting curves were taken with a Varian DMS-300 or Cary1E UV-vis spectrophotometer. A temperature probe inserted in a temperature reference cuvette adjacent to the sample was used to monitor the temperature. Samples were heated to 75°C and slowly cooled to room temperature prior to a melting experiment. Absorption at 268 nm was monitored while the temperature was increased at a rate of ~0.5°C/min. Data were taken every 0.1°C. T_m values were reproducible to ±0.5°C.

Thermodynamic analysis of triplex and duplex transitions

Complexes formed between the hairpin DNA and each single strand exhibited two transition steps. The first step was the transition from the triple helix to single strand and hairpin DNA. The second step corresponded to the transition of the hairpin DNA to its random coil form. These equilibrium reactions may be described as

$$\text{triplex} \leftrightarrow (\text{H29}) + \text{single strand} \quad \mathbf{1}$$

$$(\text{H29}) + \text{single strand} \leftrightarrow \text{coil} + \text{single strand} \quad \mathbf{2}$$

K_2 and K_3 are defined as the temperature-dependent equilibrium constants for formation of the hairpin and triplex, respectively (the reverse reaction of equations **1** and **2**). The experimental transitions were analyzed by comparing them with a theoretical melting curve determined for the coupled equilibria described by equations **1** and **2** (32).

The fraction of single-stranded oligomers that are triplex, $\theta_3(t)$, is given by

$$\theta_3(t) = K_2K_3\,(C_t/2)\,[1 - \theta_3(t)]/\{K_2K_3\,(C_t/2)\,[1 - \theta_3(t)] + K_2 + 1\} \quad \mathbf{3}$$

and the fraction of H29 molecules that are hairpins, $\theta_2(t)$, is given by

$$\theta_2(t) = \{K_2K_3\,(C_t/2)\,[1 - \theta_3(t)] + K_2\}/\{K_2K_3\,(C_t/2)\,[1 - \theta_3(t)] + K_2 + 1\}. \quad \mathbf{4}$$

C_t is the total concentration of the H29 and the single-stranded molecules. Solving equations **3** and **4** requires initial estimates of K_2 and K_3 and thus estimates of T_{m2}, ΔH°_2 and T_{m3}, ΔH°_3.

T_{m2} and ΔH°_2 were first determined using the normalized melting curve of hairpin H29 alone. The experimental fraction of H29 molecules in the hairpin conformation at temperature t (in the absence of an oligonucleotide) and the experimental derivative melting curve were compared with theoretical values of $\theta_2'(t) = K_2/(1 + K_2)$ and $d[1 - \theta_2'(t)]/dt$. Initial estimates of T_{m2} and ΔH°_2 were used to calculate $K_2(t)$ values by integration of the van't Hoff equation and adjusted to give the best fit of the theoretical curve to experiment.

Values for ΔH°_3 and T_{m3} were determined by an iterative analysis in a similar way. Initial estimates were made to the $K_3(t)$ values. $K_3(t)$ and $K_2(t)$ were then used to calculate $\theta_3(t)$ from equation **3** and $\theta_2(t)$ from equation **4**. The term $[1 - \theta_2(t) + \alpha[1 - \theta_3(t)]]/(1 + \alpha)$ was determined and its derivative plotted against temperature and compared with the normalized

experimental curve *d*Abs/*dt*. α is the ratio of the triplex/duplex transition heights. ΔH°_3 and T_{m3} values were varied to give the best fit.

The complexes formed between single strands and the tailed duplex molecules displayed single step denaturation transitions. Plots of the fraction of molecules denatured versus temperature were determined from the absorbance–temperature profiles after removing the linear portions of the upper and lower baselines. Since all single strand–tailed duplex complexes had irreversible melting transitions, thermodynamic parameters were not evaluated. We defined T_{den} as the midpoint temperature of the denaturation curve and T_{ren} as the midpoint temperature of the renaturation curve.

Gel retardation and competition assays

Triplex formation was analyzed with non-denaturing 20% polyacrylamide gels (19:1 acrylamide/bis-acrylamide) containing 1× NAE buffer (pH 5.0). A gel shift assay was employed to assess the binding of ^{32}P-labeled single strands to the H29 hairpin DNA or the DT12/6 molecules. Samples contained increasing amounts of H29 or DT12/6 molecules with a constant concentration of single strands (300 nM). Complexes were prepared by heating the DNAs to 75°C in 1× NAE buffer and cooling them to 25°C. Electrophoresis was performed for ~18 h (6 V/cm) at 25°C. The amount of radioactivity in the gel bands corresponding to the free single strand and triplex was quantified using an Ambis 4000 system (Scanalytics).

An association constant for PY12 binding to H29 was determined from gel shift data using the relation $K_3 = [T]/[PY12][H29]$ where [PY12], [H29] and [T] represent concentrations of free PY12, free H29 and the triplex. The amount of bound and free ^{32}P-labeled PY12 was determined as a function of H29 added. Taking the log of both sides of the equation for the equilibrium constant, one obtains at the point where 50% of the labeled PY12 is in the triplex the relation $\log_{10}K_3 = -\log_{10}[H29]_{0.5}$. $[H29]_{0.5}$ is the concentration of free H29 when 50% of PY12 is bound. It was determined from the total concentration of H29 added minus the concentration of triplex at the 50% point.

The gel competition assay was carried out by adding varying amounts of a competing unlabeled single-stranded oligomer (e.g. PY17) to fixed concentrations of ^{32}P-labeled PY12 (300 nM) and H29 (390 nM). The relative free energy of binding each competing single strand to H29 was determined from the plot of the decrease in the fraction of the H29·PY12 triplex (θ_t) as a function of competing single strand (Fig. 4). θ_t was experimentally determined from the band intensities:

$$\theta_t = [\text{triplex} - \text{background}]/[(\text{triplex} - \text{background}) + (\text{free strand} - \text{background})] \quad \mathbf{5}$$

From the equations relating equilibrium constants and concentrations and the total concentration of a molecule to its various forms, one obtains the theoretical relationship

$$\theta_t = 1/\{1 + ([X]\,K_x)/(K_3\,[T_x])\} \quad \mathbf{6}$$

K_x/K_3 is the ratio of binding constants of the competing single strand X and PY12 to H29, [X] is the free concentration of X and $[T_x]$ is the concentration of the triplex formed by X and H29. K_x/K_3 is evaluated from equation **6** at $\theta_t = 0.5$. The values of $[X]_{0.5}$ and $[T_x]_{0.5}$ are determined from the equations relating the concentrations of molecules.

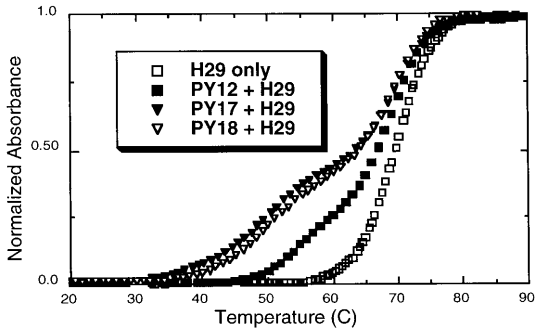

Figure 2. Normalized UV monitored melting transitions of hairpin DNA H29 (□), H29·PY12 complex (■), H29·PY17 complex (▼) and the H29·PY18 complex (▽). Sample concentrations were 1 μM each of H29 and the single strand. The solvent was 1× NAE at pH 5.0.

RESULTS AND DISCUSSION

Influence of oligonucleotide extended sequence on hairpin–oligonucleotide triplex transition

UV absorbance-monitored melting curves were obtained for complexes involving H29 and the oligonucleotides, PY12, PY17 and PY18. Figure 2 shows the melting curves of several of the DNA complexes. Denaturation–renaturation experiments indicate that the transitions occur in a reversible manner under the experimental conditions employed (data not shown). The melting curves show two step transitions allowing separate analysis of the triplex melting transition (first step) and the hairpin DNA transition (second step).

The T_m value for the triplex to hairpin plus oligonucleotide transition for PY12·H29 was 54.0°C. When 5 nt were added to the 3′-end of PY12 to produce a region complementary to the loop residues of H29, the triplex transition decreased by 4.7°C (PY17). The interaction between the hairpin loop and the 5 nt extension on PY17 destabilized rather than stabilized the triplex region. Inserting a thymine at the junction between the triplex forming bases and the 5 nt extension (PY18) produced a triplex transition that was more stable than PY17 but was still less stable than PY12. T_m values of the above triplex complexes are listed in Table 1. Analysis of the transitions of the oligomer–hairpin complexes (equations **3** and **4**) yielded T_m values for the hairpin–coil step of 69.8 ± 0.4°C. This was essentially the same as the hairpin alone. We note that consideration of the triplex strand unwinding step of the complexes yield T_m values for the hairpin–coil step that are higher than suggested by casual inspection of Figure 2.

Results from a model-dependent van't Hoff analysis (33) of the melting curves of the complexes are summarized in Table 1. The ΔH° and ΔG° value at 25°C for the triplex formed by PY12·H29 agree very well with values obtained by Roberts for a triplex with a similar structure (32) ($\Delta H^\circ = -80$ kcal/mol, $\Delta G^\circ = -15.7$ kcal/mol). The triplex studied by Roberts was the same as PY12·H29 except that the hairpin loop sequence was TTTT. The van't Hoff analysis indicates that the PY17·H29 and PY18·H29 complexes have a free energy that is 1.5–2.0 kcal/mol less stable than PY12·H29. Melting studies were also carried out with H29 and the PY19 pyrimidine strand. The result confirmed the destabilizing effect of the strands longer than PY12 (data not shown). The juxtaposition of the loop residues and the extended portion of

PY17, PY18 or PY19 appear to weaken Hoogsteen base pairing between H29 and the pyrimidine region of the single strands.

Table 1. van't Hoff analysis of melting transitions of H29 and single strands

Type of transition	T_m (°C)[a]	$\Delta H°$ (kcal/mol)[b]	$\Delta G°_{25°C}$ (kcal/mol)[c]	$\Delta S°$ (cal/K.mol)[d]
Hairpin				
H29 only	69.4	–73 ± 5	–9.5 ± 5	213 ± 17
Triplex				
H29·PY12	54.0	–76 ± 5	–15.8 ± 5	–202 ± 17
H29·PY17	49.3	–71 ± 5	–13.8 ± 5	–192 ± 17
H29·PY18	50.3	–72.4 ± 5	–14.3 ± 5	–195 ± 17

[a]T_m values were averages of two or three measurements and were reproducible to ±0.5°C.
[b]Values and uncertainties were estimated from the best fit of equations **1** and **2** to the transition curves.
[c]Free energy for the hairpin duplex was determined from $\Delta G° = \Delta H°(1 - T/T_m)$; $\Delta G°$ for the triplex was derived as described in text and from relations described by Marky and Breslauer (33).
[d]$\Delta S°$ was calculated from the equation $\Delta G° = \Delta H° - T \cdot \Delta S°$.

Gel mobility shift and gel competition assays

The gel mobility shift and competition assays were employed to provide an independent measure of the effect of the extended sequence on oligonucleotide binding to H29. The equilibrium binding of PY12 to H29 was evaluated by varying the amount of H29 in the presence of ^{32}P-labeled PY12. The amounts of free PY12 and H29·PY12 triplex were quantified on a non-denaturing gel. This information was used with the data from the gel competition experiments to determine the relative free energies between binding PY17 or PY18 and PY12 for H29.

Figure 3 shows a gel competition experiment in which PY17 was competed with PY12 for H29. When no H29 was added, all labeled PY12 migrated as free single strand (Fig. 3, lane C). In the presence of excess H29, but without a competing single strand, most of the PY12 shifted to a single triplex band (Fig. 3, lane 1). As the concentration of the competing PY17 increased, more PY12 migrated as free strands (Fig. 3, lanes 2–5). Figure 4 plots the fraction of PY12 bound to H29 (θ_t) as a function of the competing oligonucleotides PY17 and PY18. Both oligonucleotides gave similar results within the accuracy of the experiments. Analysis of the data using equation **6** gave K_x/K_3 values indicating a difference in free energy of triplex formation with PY17 or PY18 versus PY12 of $\Delta\Delta G°_{gel}$ = 1.6 kcal/mol. This value was close to the values derived from van't Hoff assays, $\Delta\Delta G°_{van't\ Hoff}$ = 1.5–2.0 kcal/mol (Table 2). Both the gel shift and melting curve results indicate that the interaction of the extended or overhanging part of the pyrimidine-rich strands with the loop destabilizes the adjacent triplex. The results do not support the notion of adjacent, stable triplex and duplex domains for the complexes between the hairpin DNA and the extended pyrimidine-rich strands.

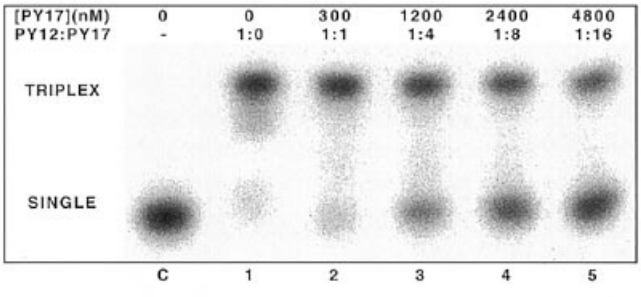

Figure 3. Gel electrophoresis competition assay. Autoradiogram of native polyacrylamide gel showing titration of unlabeled PY17 competing with ^{32}P-labeled PY12 for binding to hairpin DNA H29. Lane C, 300 nM ^{32}P-labeled PY12; lanes 1–5, 300 nM PY12 and 390 nM H29 and increasing amounts of PY17 as indicated above each lane.

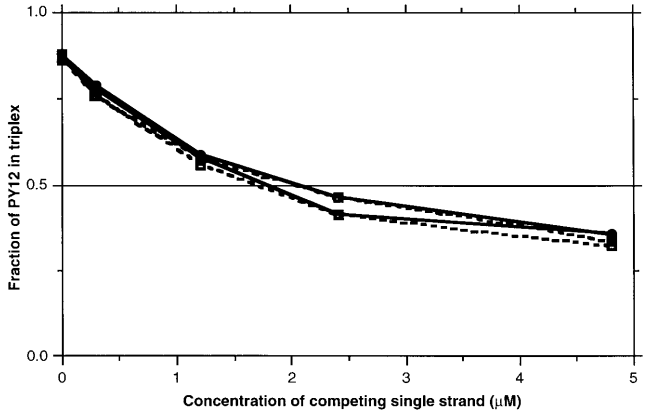

Figure 4. Data from gel competition assay experiments. The fraction of ^{32}P-labeled PY12 in the complex with H29 is plotted as a function of the concentration of competing PY17 and PY18. Dashed lines correspond to two experiments with PY17 and solid lines correspond to two experiments with PY18.

Table 2. The relative free energy for triplex formation of hairpin DNA (H29) and single strands evaluated by van't Hoff analysis of melting curves and gel competition assay

Single strand binding to H29	$\Delta\Delta G°_{gel}$ (kcal/mol)	$\Delta\Delta G°_{VH}$ (kcal/mol)
PY12	0	0
PY17	1.6	2.0
PY18	1.6	1.5

It is worth noting that the value of K_3 determined from the gel shift assay yielded a $\Delta G°$ value for the PY12·H29 triplex at 25°C that was 6.5 kcal/mol lower than the value determined from the van't Hoff analysis. Although several potential explanations for this discrepancy are possible, the reason is uncertain. The van't Hoff determination of $\Delta H°$ from the melting curve may be inaccurate if the assumptions of a two-state transition and/or temperature-independent extrapolation of $\Delta H°$ are incorrect. However, van't Hoff derived values and calorimetric measurements for similar systems agree well with our value for the pH 5.0 solvent

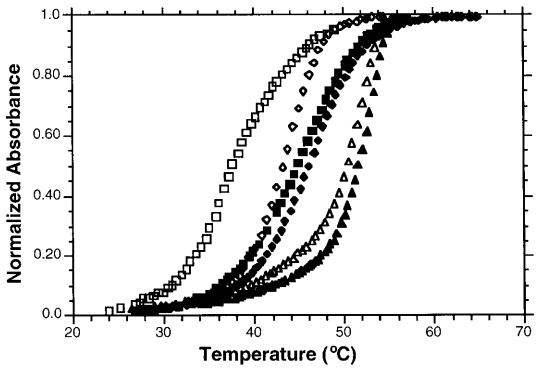

Figure 5. UV-monitored denaturation transitions of DNA complexes involving DT12/6 and DX12 in 1× NAE solvent at pH 5.0. Samples had 1 µM of the duplex or 1 µM each of duplex and single strand. □, DT12/6 only; ◇, PY12·DX12; ■, PY12·DT12/6; ◆, PY17·DT12/6; Δ, PY18·DT12/6; ▲, PY20·DT12/6.

(34,35). The influence of triplex formation kinetics was examined by extending the annealing time to 2 h in the gel experiments. This did not alter the results. Potential reasons for the discrepancy are differences in the single-stranded states at the higher thermal energy of the melting event versus the measurement at room temperature (2) or alteration of the triplex–hairpin equilibrium due to gel electrophoresis.

Complexes of single strands and DT12/6

Thermal denaturation curves of four complexes of DT12/6 and single-stranded oligomers are shown in Figure 5. All melting curves of the three-stranded complexes showed single cooperative transitions indicating that the complexes dissociated into three single strands in one step. The midpoint temperature of the denaturation curves for all complexes examined are presented in Table 3. T_{den} for the DT12/6 molecule alone was 37.6°C. When DT12/6 formed a complex with PY12 there was a 7.2°C increase in T_{den}. This increase in thermal stability demonstrates the stabilizing effect of the Hoogsteen base paired PY12 on the duplex (36). A similar increase in stability was noted for the PY12 complex with DX12, the blunt-ended duplex. The T_{den} value of the PY17·DT12/6 complex was 46°C, 1.2°C higher than the PY12·DT12/6 complex. Unlike the loop sequence of the H29 hairpin DNA, the single-stranded end of DT12/6 interacted favorably with the five Watson–Crick complementary bases on the 3′-end of PY17.

The effect of adding one or two unpaired thymines at the junction of the triplex and duplex binding domains of PY17 was examined using PY18 and PY19. These two single strands can form the same 12 Hoogsteen triplex pairs and five Watson–Crick base pairs as PY17 (Fig. 1). The addition of the thymines at the junction enhanced the stability of the complex. T_{den} values of PY18·DT12/6 and PY19·DT12/6 were 4.2 and 5.7°C higher than the denaturation midpoint of PY17·DT12/6. The effect of adding one additional Watson–Crick complementary base on the 3′-end of PY19 was examined with PY20. The one additional terminal A·T pair did not have a significant effect on denaturation.

The effect of replacing two G·C base pairs in the dangling end region with G·T mismatches was examined with complexes involving DT12/6M with PY18 and PY20. T_{den} for PY18·DT12/6 M and PY20·DT12/6M were 44.6 and 43.1°C, respectively, and were ~6–8°C lower in stability than the analogous DT12/6 base paired complexes (Table 3). This demonstrated the expected destabilizing effect of the mismatches. The influence of GC composition in the duplex region was examined using the DNA DT12/6G. All 6 nt of the dangling end were either G or C and were complementary to the six bases on the 3′-end of PY20G (Fig. 1). T_{den} for this complex, PY20G·DT12/6G, was 54.5°C, or 3°C higher than PY20·DT12/6. The above results are consistent with adjoining duplex and triplex base pairing in these complexes.

Table 3. Denaturation and renaturation midpoint temperature of various DNA complexes[a]

Type of complex	T_{den} (°C)[b]	T_{ren} (°C)[b]
DX12 only	36.3	36.5
DT12/6 only	37.6	37.6
DX12 + PY12	43.2	42.1
DT12/6 + PY12	44.8	41.5
DT12/6 + PY17	46.0	40.6
DT12/6 + PY18	50.2	41.7
DT12/6 + PY19	51.7	42.8
DT12/6 + PY20	51.4	43.4
DT12/6M + PY18	44.6	41.3
DT12/6M + PY20	43.1	41.5
DT12/6G + PY20G	54.5	45.5

[a]Each single strand was mixed with a duplex (DT12/6, DX12, DT12/6M or DT12/6G) to form the complexes indicated.
[b]T_{den}, denaturation; T_{ren}, renaturation. All T_{den} and T_{ren} values were an average of two or three UV transition curves. Repeat experiments were within ±0.5°C of each other.

Thermal denaturation and renaturation curves of the bimolecular complexes of DT12/6 with PY12, PY17 and PY18 are shown in Figure 6. Unlike the melting transitions of H29 and the single strands, the transitions were not reversible. Although the denaturation temperatures of DT12/6 and the single strands increased with the stability of the duplex region, the midpoint temperatures of renaturation curves were essentially the same for the complexes involving PY12, PY17 and PY18 (Table 3). The average T_{ren} and standard deviation for the four complexes were 41.3 ± 0.4°C. Similar T_{ren} values were also obtained for the two complexes involving DT12/6M. The 12 Watson–Crick base pairs between R12 and Y18 or Y18M are common to the complexes. This implies that this duplex region is the likely nucleation site for renaturation. The slightly higher T_{ren} values of PY19·DT12/6, PY20·DT12/6 and PY20G·DT12/6G may correlate with increased stability of the duplex segment formed at the dangling ends. Watson–Crick base pairing at the dangling end appears to also influence renaturation of the three strands.

Gel mobility shift assay of triplex–duplex formation with DT12/6

The gel mobility shift assay was employed to provide a different approach for characterizing the association of the single strands with the DT12/6 molecule. Figure 7 shows the effect of adding

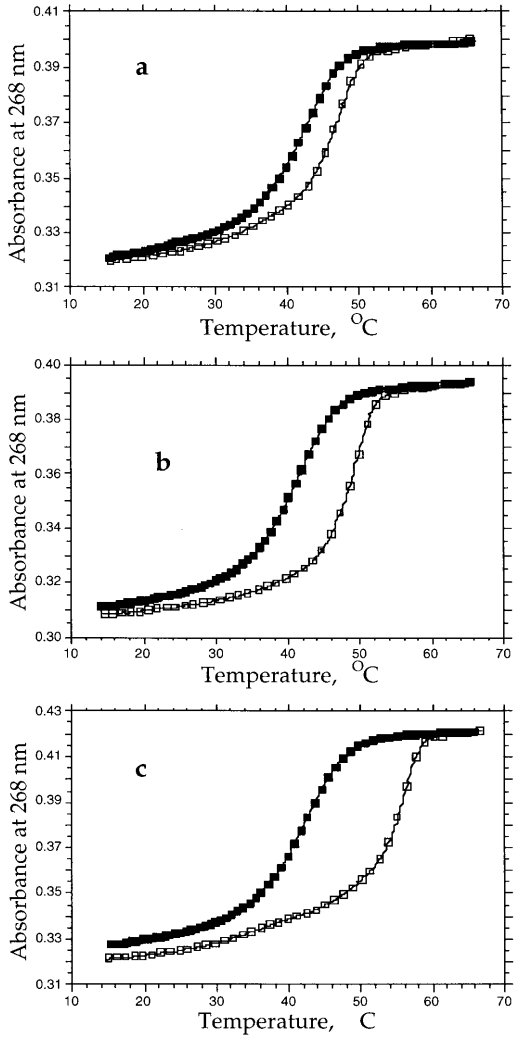

Figure 6. Denaturation and renaturation curves of (**a**) PY12·DT12/6, (**b**) PY17·DT12/6 and (**c**) PY18·DT12/6. Denaturation curves are indicated by (□) and renaturation curves are indicated by (■). Experimental conditions as described in Figure 5 and in text.

increasing amounts of unlabeled DT12/6 duplex on the gel mobility of ^{32}P-labeled PY18 at 300 nM. Two distinct bands were observed. The lower one corresponds to the free single strand, PY18, and the upper band corresponds to the complex of PY18 and DT12/6. The concentration of free PY18 decreases in an approximately linear fashion with increasing amounts of DT12/6. Essentially all of the PY18 molecules migrated as a complex when the ratio of DT12/6 to PY18 reached 0.8:1. The saturation of the PY18 molecules at a DT12/6 concentration below a 1:1 ratio is probably due to inaccuracies in estimating the concentrations. The single upper band indicates that a 1:1 complex forms between DT12/6 and the single strand. Titration experiments similar to Figure 7 with PY18 replaced by PY12, PY17 or PY20 gave similar results (not shown). It was not possible to distinguish different affinities among the single strands for DT12/6 from these experiments. This result is similar in outcome to the thermal renaturation studies and appears to reflect the high to low temperature complex formation.

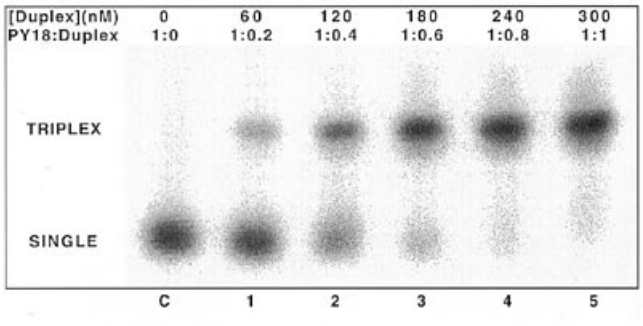

Figure 7. The autoradiogram of a gel mobility shift assay in which increasing amounts of unlabeled DT12/6 was added to ^{32}P-labeled PY18 at 300 nM. Lane C, PY18 alone; lanes 1–5, PY18 mixed with amounts of DT12/6 indicated above each lane. Bands corresponding to the triplex complex and free PY18 are indicated.

The above studies indicate that a DNA oligonucleotide and a duplex molecule containing a dangling end can form a stable duplex–triplex junction. Insertion of one or two thymines at the junction increased the stability of the complexes to denaturation. Alteration of the bases in the dangling end region effects the stability of the complex in a manner expected for Watson–Crick base pairs. The findings are consistent with results obtained by Francois and Hélène (26) who examined a related but different model system. The observation that the single strand overhang decreases rather than increases the triplex melting curve of the hairpin DNA suggests that conformational constraints of the loop sequence do not allow the extended single strand to form a stable duplex–triplex structure.

ACKNOWLEDGEMENT

We thank April Chester for her assistance with some experiments.

REFERENCES

1 Mirkin,S.M. and Frank-Kamenetskii,M.D. (1994) *Annu. Rev. Biophys. Biomol. Struct.*, **23**, 541–576.
2 Plum,G.E., Pilch,D., Singleton,S.F. and Breslauer,K.J. (1995) *Annu. Rev. Biophys. Biomol. Struct.*, **24**, 319–350.
3 Mirkin,S.M., Lyamichev,B.I., Drushlyak,K.N., Dobrynin,V.N., Flippov,S.A. and Frank-Kamenetskii,M.D. (1987) *Nature*, **330**, 495–497.
4 Htun,H. and Dahlberg,J.E. (1989) *Science*, **243**, 1571–1576.
5 Schimizu,M., Hanvey,J.C. and Wells,R.D., (1989) *J. Biol. Chem.*, **264**, 5944–5949.
6 Ussery,D.W. and Sinden,R.R. (1993) *Biochemistry*, **32**, 6206–6213.
7 Strobel,S.A., Doucette-Stamm,L.A., Riba,L., Housman,D.E. and Dervan,P.B. (1991) *Science*, **254**, 1639–1642.
8 Strobel,S.A. and Dervan,P.B. (1992) *Methods Enzymol.*, **216**, 309–321.
9 Cooney,M., Czernuszewicz,G., Postel,E.H., Flint,S.J. and Hogan,M.E. (1988) *Science*, **241**, 456–459.
10 Alunni-Fabbroni,M., Manfioletti,G., Manzini,G. and Xodo,L.E. (1994) *Eur. J. Biochem.*, **226**, 831–839.
11 Young,S.L., Krawczyk,S.H., Matteucci,M.D. and Toole,J.J. (1991) *Proc. Natl Acad. Sci. USA*, **88**, 10023–10100.
12 Duval-Valentin,G., Thoung,N.T. and Hélène,C. (1992) *Proc. Natl Acad. Sci. USA*, **89**, 504–508.
13 Dayn,A., Samadashwily,G.M. and Mirkin,S.M. (1992) *Proc. Natl Acad. Sci. USA*, **89**, 11406–11410.
14 Mergny,J.I., Duval-Valentin,G., Nguyen,C.H., Perrouault,L., Faucon,B., Rougee,M., Montenay-Garetier,T., Bisagni,E. and Hélène,C. (1992) *Science*, **256**, 1681–1684.
15 Maher,L.J.I., Dervan,P.B. and Wold,B. (1992) *Biochemistry*, **31**, 70–81.

16 Giovannangeli,C., Perrouault,L., Escudé,C., Thuong,N. and Hélène,C. (1996) *Biochemistry*, **35**, 10539–10548.
17 Ono,A., Tso,P.O.P. and Kan,L.-S. (1991) *J. Am. Chem. Soc.*, **113**, 4032–4033.
18 Miller,P.S., Bhan,P., Cushman,C.D. and Trapane,T.L. (1992) *Biochemistry*, **31**, 6788–6793.
19 Jetter,M.C. and Hobbs,F.W. (1993) *Biochemistry*, **32**, 3249–3254.
20 Giovannangeli,C., Thuong,N.T. and Hélène,C. (1993) *Proc. Natl Acad. Sci. USA*, **90**, 10013–10017.
21 Escude,C., Giovannangeli,C., Sun,J.S., Lloyd,D.H., Chen,J.K., Graznov,S.M., Garestier,T. and Hélène,C. (1996) *Proc. Natl Acad. Sci. USA*, **93**, 4365–4369.
22 Sun,J.S., Giovannangeli,C., Francois,J.C., Kurfurst,R., Montenay-Garestier,T., Asseline,U., Saison-Behmoaras,T., Thuong,N.T. and Hélène,C. (1991) *Proc. Natl Acad. Sci. USA*, **88**, 6023–6027.
23 Kukreti,S., Sun,J.S., Garestier,T. and Hélène,C. (1997) *Nucleic Acids Res.*, **25**, 4265–4270.
24 Roberts,R.W. and Crothers,D.M. (1991) *Proc. Natl Acad. Sci. USA*, **88**, 9397–9401.
25 Roberts,R.W. and Crothers,D.M. (1996) *Proc. Natl Acad. Sci. USA*, **93**, 4320–4325.
26 Francois,J.C. and Hélène,C. (1995) *Biochemistry*, **34**, 65–72.
27 Wang,S., Booher,M.A. and Kool,E.T. (1994) *Biochemistry*, **33**, 4639–4644.
28 Booher,M.A., Wang,S. and Kool,E.T. (1994) *Biochemistry*, **33**, 4645–4651.
29 Roberts,R.W. and Crothers,D.M., (1996) *J. Mol. Biol.*, **260**, 135–146.
30 Mundt,A.A., Crouch,G.J. and Eaton,E.B. (1997) *Biochemistry*, **36**, 13004–13009.
31 Cantor,C.R., Warshaw,M. and Shapiro,H. (1970) *Biopolymers*, **9**, 1059–1077.
32 Roberts,R.W. (1993) *Physical Chemistry of Nucleic Acid Triple Helices*, PhD thesis, Yale University, New Haven, CT.
33 Marky,L.A. and Breslauer,K. (1987) *Biopolymers*, **26**, 1601–1620.
34 Volker,J., Botes,D.P., Lindsey,G.G. and Klump,H.H. (1993) *J. Mol. Biol.*, **230**, 1278–1290.
35 Manzini,G., Xodo,L.E., Gasparotto,D., Quadrifoglio,F., van der Marel,G.A. and van Boom,J.H. (1990) *J. Mol. Biol.*, **213**, 833–843.
36 Kandimalla,E.R. and Agrawal,S. (1994) *Gene*, **149**, 115–121.